Data-Driven Disturbance Estimation and Control with Application to Blood Glucose Regulation

(Article begins on next page)

09 March 2021

Data-driven disturbance estimation and control with application to blood glucose regulation

Carlo Novara, Ivana Rabbone, Davide Tinti

Abstract—**A data-driven control approach for nonlinear systems is proposed, called Data-Driven Estimation and Control (D2EC), which combines a disturbance estimator and a nonlinear control algorithm. The estimator provides a signal representing the unknown disturbances affecting the plant to control. This signal is used by the control algorithm to improve its performance. A real-data study is presented, concerned with regulation of blood glucose concentration in type 1 diabetic patients. Preliminary tests of the the D2EC approach are also carried out using a diabetic patient simulator, obtained from a revised version of the well-known UVA/Padova model. Both the real-data and the simulator-based studies indicate that the proposed approach has the potential to become an effective tool in the context of diabetes treatment and, more in general, in the biomedical field, where accurate first-principle models can seldom be found and relevant disturbances are present.**

I. INTRODUCTION

Controlling a real-world system may be hard for several reasons. Among the most relevant difficulties, we can distinguish the following three: First, the plant to control may be highly nonlinear, so that linear control techniques are inappropriate. Second, the plant may be not well known or too complex to model using first-principle equations. Third, non-measured disturbances may be present, affecting considerably the plant behavior.

These issues may prevent the classical control approaches from working properly. In the nonlinear case, examples are Feedback Linearization [1], [2], Lyapunov function based control [3], [4] and standard Nonlinear Model Predictive Control (NMPC), [5], [6], [7]. These approaches typically assume that an accurate first-principle model describing the system dynamics is available and that the involved disturbances are sufficiently small. However, in many practical situations, deriving an accurate first-principle model is difficult: the system dynamics may be not well understood and/or too complex; there may be parameters that are difficult to measure/estimate. In these situations, only approximate/inaccurate first-principle models can be derived. Moreover, the presence of unmeasured disturbances may lead to a significant degradation of the plant performance.

Robust methods have been developed to deal with the issue of approximate modeling, [8], [9], [10]. However, deriving the required uncertainty models is not easy even for Linear Time Invariant (LTI) systems (see e.g. [11] and the references therein), and is still an open problem in the case of nonlinear systems.

C. Novara is with Politecnico di Torino, Italy. I. Rabbone and D. Tinti are with Ospedale Sant'Anna, Torino, Italy. Email: `carlo.novara@polito`, `ivana.rabbone@unito.it`, `davide.tinti@unito.it`.

Active Disturbance Rejection Control (ADRC) and Embedded Model Control (EMC) proved to be quite effective methods to deal with significant disturbances, [12], [13]. These methods rely on the knowledge of the plant physical model structure and, in particular, on the assumption that the plant model is affine in the control input (analogously to what done in Feedback Linearization). However, such assumptions on the model structure may not hold in several real situations.

A change of paradigm is represented by data-driven methods, which can be roughly classified in two main categories (in the following, only works related to nonlinear systems are cited): indirect techniques, which employ the data to identify some model to use for control, [14], [15], [16], [17], [18], [19], [20], [21], [22], [23]; direct techniques, which obtain the controller directly from the available input-output data, [24], [25], [26], [27], [28], [29]. There is a third category, represented by adaptive/reinforcement learning techniques, where the controller (or the model or both of them) is tuned using the data measured during online operations, [18], [30], [31], [32], [33], [34], [35]; since adaptive/reinforcement learning techniques can be employed within any more general approach, this latter category can be seen as a subcategory of the previous two.

Data-driven methods can effectively deal with highly nonlinear systems and are not affected by the problem of approximate modeling, since the controller is synthesized from data, without requiring a first-principle model. Notwithstanding these nice features, serious problems may arise in the presence of relevant disturbances. Indeed, these disturbances may not allow a sufficiently accurate model identification (indirect techniques) and/or an effective control design (indirect and direct techniques). Even in cases where some effective model and/or controller have been found, the disturbances, if not properly accounted for, may yield significant degradations of the control performance.

In this paper, a data-driven control design approach for nonlinear systems is proposed, allowing us to overcome the aforementioned problems. The approach combines the blind identification technique of [36] and the Nonlinear Inversion Control (NIC) algorithm of [37], [38]. The blind identification technique allows us to derive an estimator of the unknown disturbances, whose output is used by the NIC algorithm to improve its control performance. The overall controller is composed by an estimator and a control algorithm, and both of them are synthesized from experimental data, without requiring a first-principle model. The method is here named Data-Driven Estimation and Control (D2EC).

Thanks to these features, the D2EC approach may be particularly effective in the biomedical field, for the treatment of various diseases, where deriving accurate physiological models is difficult, there is a strong variability among the patient population and the disturbances strongly affect the patient conditions. The D2EC approach allows indeed the design of treatment strategies that are personalized for each patient, avoiding the population variability problem. It does not require accurate physiological models: control design can be carried out from a set of data acquired in a preliminary phase of the treatment. Disturbances are estimated on-line in order to improve the control performance.

In summary, the main contributions of this paper are two. The first one consists in the idea of combining a data-driven disturbance estimator and a data-driven control algorithm. To the best of our knowledge, no methods can be found in the literature using a combination of a disturbance estimator and a nonlinear controller, where both these elements are designed from data. Note also that the proposed technique for designing the disturbance estimator is novel. Such a technique is based on a model identified by the blind identification approach of [36] and allows us to build an estimator with a NARX (Nonlinear AutoRegressive with eXogenous inputs) structure, that is able to recover the unknown disturbance in real-time. The control algorithm is an extension of the one proposed in [38] and the related closed-loop stability analysis is novel, in the sense that it accounts for the estimator in the loop, that is not present in [37], [38].

The second contribution is a real-data study, concerning regulation of blood glucose concentration in type 1 diabetic patients. First, a model of a diabetic patient is identified from a subset of the available experimental data. This model represents the (unknown) patient, for which a glucose regulator has to be designed. In other words, this patient model is used instead of a real patient (future activities will hopefully be devoted to test the D2EC approach in clinical trials with real patients). Then, a D2EC therapy control strategy is designed using a given set of data, and afterward tested using fresh data, not previously used for controller/estimator design. This study shows that the D2EC strategy is effective in regulating the blood glucose concentration of the patient model, yielding a significantly better treatment quality with respect to a "manual" strategy, where the insulin is injected by the patient on the basis of his/hers experience and of the indications coming from a semi-automated glucose regulation device. The treatment quality of the D2EC strategy is comparable with the one provided by an ideal NMPC controller, which uses exact information on the true patient model and on the disturbance. In the context of blood glucose regulation, the D2EC approach is also tested using a diabetic patient simulator, obtained from a revised version of the well-known UVA/Padova model. The obtained results are similar to those obtained using our data-driven models, confirming that the approach can work, also when the system to control is characterized by a completely different model structure and a completely different class of nonlinearities with respect to those used

by the D2EC approach.

II. NOTATION

A column vector $x \in \mathbb{R}^{n_x \times 1}$ is denoted by $x = (x_1, \ldots, x_{n_x})$. A row vector $x \in \mathbb{R}^{1 \times n_x}$ is denoted by $x = [x_1, \ldots, x_{n_x}] = (x_1, \ldots, x_{n_x})^\top$, where $\top$ indicates the transpose.

A discrete-time signal (i.e. a sequence of vectors) is denoted with the bold style: $\boldsymbol{x} = (x_1, x_2, \ldots)$, where $x_t \in \mathbb{R}^{n_x \times 1}$ and $t = 1, 2, \ldots$ indicates the discrete time; $x_{i,t}$ is the ith component of the signal $\boldsymbol{x}$ at time t.

The ℓ_p norm of a vector $x = (x_1, \ldots, x_{n_x})$ is defined as

$$\|x\|_p \doteq \begin{cases} \left(\sum_{i=1}^{n_x} |x_i|^p\right)^{\frac{1}{p}}, & p < \infty, \\ \max_i |x_i|, & p = \infty. \end{cases}$$

The ℓ_0 quasi-norm of a vector is defined as the number of its non-zero components.

The ℓ_p norm of a signal $\boldsymbol{x} = (x_1, x_2, \ldots)$ is defined as

$$\|\boldsymbol{x}\|_p \doteq \begin{cases} \left(\sum_{t=1}^{\infty} \sum_{i=1}^{n_x} |x_{i,t}|^p\right)^{\frac{1}{p}}, & p < \infty, \\ \max_{i,t} |x_{i,t}|, & p = \infty, \end{cases}$$

where $x_{i,t}$ is the ith component of the signal $\boldsymbol{x}$ at time t.

The L_p norm of a function with domain $X \subseteq \mathbb{R}^{n_x}$ and codomain in $\mathbb{R}$, is defined as

$$\|f\|_p \doteq \begin{cases} \left[\int_X \|f(x)\|_p^p \, dx\right]^{\frac{1}{p}}, & p \in (1, \infty), \\ \text{ess sup}_{x \in X} \|f(x)\|_\infty, & p = \infty. \end{cases}$$

These norms give rise to the well-known ℓ_p and L_p Banach spaces. For simplicity, the norms without the subscript are defined as $\|\cdot\| \doteq \|\cdot\|_\infty$ for both the ℓ_∞ and L_∞ cases.

III. PROBLEM FORMULATION AND PROPOSED APPROACH

Consider a nonlinear discrete-time system of the form

$$y_t = h\left(u_t^-, y_t^-\right) + \xi_t \qquad (1)$$
$$u_t^- \doteq (u_{t-1}, \ldots, u_{t-n})$$
$$y_t^- \doteq (y_{t-1}, \ldots, y_{t-n})$$

where $u_t \in U \subset \mathbb{R}$ is the input, $y_t \in \mathbb{R}$ is the output, $\xi_t \in \Xi \subset \mathbb{R}$ is an unknown disturbance, n is the system order, $t \in \mathbb{Z}$ is the time index, $h : \mathbb{R}^{2n} \to \mathbb{R}$, $U \doteq \{u \in \mathbb{R} : |u| \leq \bar{u}\}$ and $\Xi \doteq \{\xi \in \mathbb{R} : |\xi| \leq \bar{\xi}\}$.

Suppose that the system (1) is unknown, but a set of noise-corrupted measurements is available:

$$DS \doteq \{\tilde{u}_t, \tilde{y}_t\}_{t=1-n-L}^{0} \qquad (2)$$

where $\tilde{u}_t \in U$, $\tilde{y}_t \in Y$, $Y \subset \mathbb{R}$ is a compact set, and the tilde is used to indicate the collected data.

Let $\mathcal{Y}^0 \subseteq R^n$ be a set of initial conditions of interest, $R \subset \mathbb{R}$ a compact set, $\mathcal{R} \doteq \{\boldsymbol{r} = (r_1, r_2, \ldots) : r_t \in R, \forall t\}$ a set of output sequences of interest and $\Xi \doteq \{\boldsymbol{\xi} = (\xi_1, \xi_2, \ldots) : \xi_t \in \Xi, \forall t\}$ the set of all possible disturbance sequences.

The problem is to design a controller for the system (1) such that, for any $\boldsymbol{\xi} = (\xi_1, \xi_2, \ldots) \in \Xi$, and for any initial condition $y_0^- \in \mathcal{Y}^0$, the output sequence $\boldsymbol{y} = (y_1, y_2, \ldots)$ of the controlled system tracks any reference sequence $\boldsymbol{r} = (r_1, r_2, \ldots) \in \mathcal{R}$.

In this paper, we propose an approach to this problem, that we call Data-Driven Estimation and Control (D2EC), based on three main steps:

1) Data-driven estimator design (off-line). A disturbance estimator is synthesized off-line from the data (2), allowing us to obtain an on-line estimate of the disturbance ξ_t in (1).
2) Data-driven identification of a prediction model (off-line). A prediction model for the plant (1) is identified off-line from the data (2). This model uses on-line the estimator output as an input, in order to improve the prediction accuracy.
3) Model inversion control (on-line). The control law is obtained by on-line inversion of the prediction model, via efficient optimization.

The complete control system structure is depicted in Figure 1, where "plant" is the system (1), H is the disturbance estimator, K is the controller, y_t is the output, $r_{t+\tau}$ is a reference value, u_t^* is the command input, ξ_t is the true disturbance and $\hat{\xi}_t$ is the disturbance estimate.
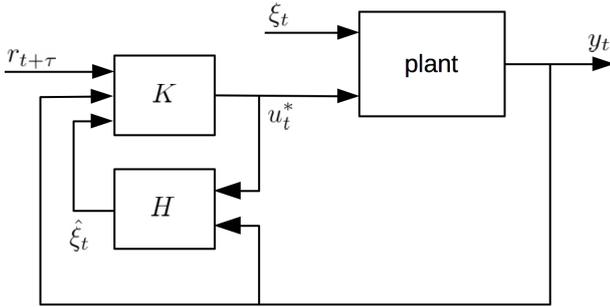

Figure 1. Closed-loop control system.

IV. Estimator design via blind identification

In this section, the blind identification method of [36] is summarized and suitably adapted for the present context. Then, a novel disturbance estimator is derived, based on the model obtained using this method. The estimator output is used as an input of the prediction model presented in the next section, to improve its prediction accuracy.

The method of [36] allows us to derive models of the form (1), with estimates $\hat{h}$ and $\hat{\xi}_t^{nc}$ of both the function h and the disturbance ξ_t. Such estimates are given by

$$\begin{aligned}
\hat{h}\left(w_t^-\right) &= \sum_{i=1}^{P} a_i \chi_i\left(w_t^-\right) \\
\hat{\xi}_t^{nc} &= \sum_{i=1}^{M} b_i \psi_i(t)
\end{aligned} \tag{3}$$

where $w_t^- \doteq \left(u_t^-, y_t^-\right) = (u_{t-1}, \ldots, u_{t-n}, y_{t-1}, \ldots, y_{t-n})$, $\chi_i : \mathbb{R}^{2n} \to \mathbb{R}$ and $\psi_i : \mathbb{Z} \to \mathbb{R}$ are known basis functions, and $a_i \in \mathbb{R}$ and $b_i \in \mathbb{R}$ are parameters to identify.

The choice of the basis functions is clearly an important step of the identification process, [39], [40], [41]. In some

cases of practical interest, the basis functions may be known a priori. In other cases, the basis functions are not known and their choice can be carried out considering the numerous options available in the literature (e.g. Gaussian, exponential, sigmoidal, wavelet, polynomial, trigonometric). Here, we adopt this latter approach, considering large sets $\{\phi_i\}_{i=1}^{N}$ and $\{\psi_i\}_{i=1}^{M}$ of basis functions, resulting in over-parametrized models (3). As shown below, selection of the most appropriate functions within these sets is carried out by means of ℓ_1-norm minimization, [42], [43], [44], [45].

According to (1), the data (2) can be described as

$$\tilde{y}_t = h\left(\tilde{w}_t^-\right) + \xi_t = \hat{h}\left(\tilde{w}_t^-\right) + e_t, \ t = 1 - L, \ldots, 0 \tag{4}$$

where $\tilde{w}_t^- \doteq (\tilde{u}_t^-, \tilde{y}_t^-) = (\tilde{u}_{t-1}, \ldots, \tilde{u}_{t-n}, \tilde{y}_{t-1}, \ldots, \tilde{y}_{t-n})$ is the measured regressor, and e_t is an error/disturbance term including ξ_t, the measurement errors corrupting y_t and w_t^-, and possible modeling errors due to the parametrization (3). Following a Set Membership philosophy ([46], [47], [48], [49]), the sequence $e \doteq (e_{1-L}, \ldots, e_0)$ is assumed bounded:

$$\|e\| \le \varepsilon \tag{5}$$

for some $\varepsilon \ge 0$. From this assumption and equations (3) and (4), it follows that

$$\|Z - \Lambda a - \Psi b\| \le \varepsilon \tag{6}$$

where

$$\begin{aligned}
Z &\doteq (\tilde{y}_{1-L}, \ldots, \tilde{y}_0) \in \mathbb{R}^{L \times 1} \\
a &\doteq (a_1, \ldots, a_P) \in \mathbb{R}^{P \times 1} \\
b &\doteq (b_1, \ldots, b_M) \in \mathbb{R}^{M \times 1}
\end{aligned}$$

$$\Lambda \doteq \begin{bmatrix} \chi_1\left(\tilde{w}_{1-L}^-\right) & \cdots & \chi_N\left(\tilde{w}_{1-L}^-\right) \\ \vdots & \ddots & \vdots \\ \chi_1\left(\tilde{w}_0^-\right) & \cdots & \chi_N\left(\tilde{w}_0^-\right) \end{bmatrix} \in \mathbb{R}^{L \times P}$$

$$\Psi \doteq \begin{bmatrix} \psi_1(1-L) & \cdots & \psi_M(1-L) \\ \vdots & \ddots & \vdots \\ \psi_1(0) & \cdots & \psi_M(0) \end{bmatrix} \in \mathbb{R}^{L \times M}. \tag{7}$$

The vectors $a \in \mathbb{R}^P$ and $b \in \mathbb{R}^M$, whose entries are the parameters of the model (3), are identified by means of the following convex algorithm.

Identification algorithm 1: $(a, b) = \text{id\_blind\_1}(DS, \varepsilon)$.

Identification of the parameter vectors a and b is carried out solving the following convex optimization problem:

$$\begin{aligned}
(a, b) &= \arg\min_{(\hat{a}, \hat{b})} \|\hat{a}\|_1 + \left\|\hat{b}\right\|_1 \\
\text{s.t.} \quad &\left\|Z - \Lambda \hat{a} - \Psi \hat{b}\right\| \le \varepsilon.
\end{aligned} \tag{8}$$

The rationale behind this algorithm can be explained as follows:

1) The constraint $\|Z - \Lambda a - \Psi b\| \le \varepsilon$ guarantees consistency between the measured data and the prior assumption (6). If the ε bound is true, then although there are multiple a and b that satisfy the ε bound,

a much smaller subset of these will minimize the ℓ_1 norm objective function. In fact, under very mild assumptions, as given in [45], this set is a singleton, and the solution is guaranteed to be unique. However, an incorrect choice for ε has the effect of biasing the parameter estimates, so it should be chosen using a validation procedure such as in [50].

2) ℓ_1-norm minimization of a and b is used to enforce sparsity of the coefficient vectors a and b, [51], [45], [43], [44].

   a) Sparsity of a is useful to obtain a model with a low complexity, i.e., described by a limited number of basis functions (those corresponding to non-zero entries of a), selected within a "large" set.

   b) Sparsity of b is important to correctly recover the true disturbance ξ_t in situations where this signal can be represented as a superposition of a small number of basis functions (for example, these functions can represent the meals in a diabetic patient, see Section VII).

Conditions verifiable in practice, under which the proposed ℓ_1 minimization problem gives a maximally sparse solution can be obtained by minor modifications of Theorem 1 in [52]. Under these conditions, the minimization problem is able to provide a low complexity model $\hat{h}$ (i.e., with a minimum number of basis functions) and to correctly find the most appropriate basis functions that define the disturbance ξ_t.

Remark 1: The parameter ε in (5) can be systematically estimated using the validation procedure in [50]. This procedure relies on the so-called validation surface, i.e., a surface constructed from the available data, that separates the parameter values that are validated by the data from those that are not. The parameters (ε in this case) are chosen in the validated region by means of a simple criterion which, in the present context, can be suitably defined to obtain an optimal trade-off between model accuracy and complexity. $\square$

Remark 2: The identification algorithm proposed above can be used also in cases where a reliable system model $\hat{h}$ is already available and it is of interest to recover the disturbance ξ_k. This can be done solving the optimization problem (8) only with respect to b, being a the coefficient vector of $\hat{h}$ (see Section VII-E, where this technique is used for estimating the unknown disturbance, given mainly by meals and physical activities, in diabetic patients). $\square$

Remark 3: When a large number of parameters/basis functions is used in a model, the issue of over-fitting may arise. In practice, it may happen that the model is extremely accurate on the data used for its identification but has a poor generalization capability, resulting in a low accuracy when applied to fresh data. To avoid this issue, two operations can be useful: (i) including a regularization term in the model identification algorithm; (ii) performing extensive validations of the model on data not used for identification. Our identification algorithms (one presented in this section, the other presented in Section V) feature ℓ_1 regularization terms, allowing also a reduction of the model complexity. Moreover, in the application presented below about blood glucose regulation in diabetic patients, the identified models are validated using fresh data in order to have a certain level of confidence that no over-fitting occurs. $\square$

Solving the optimization problem (8) and using the identified parameters in (3), a non-causal estimate of the unknown disturbance is derived: the estimate $\hat{\xi}_t^{nc}$ at time t is obtained using the past, current and future data. Obviously, non-causal estimates cannot be performed on-line. Hence, a causal estimate is obtained by means of the following estimation algorithm.

Estimation algorithm 1: $\hat{\xi}_t = H\left(w_t^-, y_t\right)$.

$$\hat{\xi}_t = H\left(w_t^-, y_t\right) \doteq y_t - \hat{h}\left(w_t^-\right) \qquad (9)$$

where $\hat{\xi}_t$ is the estimate of the unknown disturbance ξ_t affecting the system (1), y_t is the measured output, $w_t^- \doteq \left(u_t^-, y_t^-\right)$, and u_t^- and y_t^- are the corresponding measured input and output regressors. The function $\hat{h}$ in (9) is given by (3), where the parameters a_i are identified by means of algorithm 1.

Note that the estimator H in (9) is characterized by a NARX (Nonlinear AutoRegressive with eXogenous inputs) structure. Future research activities will be devoted to investigate a NARMAX (Nonlinear AutoRegressive Moving Average with eXogenous inputs) structure, which could help to improve the estimator performance.

V. PREDICTION MODEL

In this section, a prediction model for the system (1) is identified from the data (2). This model uses the estimator output as an input, in order to improve its prediction accuracy. The control law presented in the next section is obtained through on-line inversion of the prediction model, via efficient optimization.

Consider that the system (1) can be represented in the τ-step ahead prediction form

$$y_{t+\tau} = g\left(u_t^+, u_t^-, y_t^-, \xi_t^v\right) \qquad (10)$$
$$u_t^+ \doteq (u_{t+\tau-1}, \ldots, u_t)$$
$$\xi_t^v \doteq (\xi_{t+\tau-1}, \ldots, \xi_{t-n})$$

where $g\left(\cdot\right) \doteq h^{\tau+1}\left(\cdot\right)$ is obtained by $\tau+1$ iterations of equation (1) and τ is the prediction horizon.

We introduce a prediction model, obtained as an approximation of the system (10), of the form

$$\hat{y}_{t+\tau} = f\left(u_t, q_t^-\right) \qquad (11)$$
$$q_t^- \doteq \left(u_t^-, y_t^-, \hat{\xi}_t^-\right)$$
$$\hat{\xi}_t^- \doteq \left(\hat{\xi}_{t-1}, \ldots, \hat{\xi}_{t-n}\right)$$

where $f : \mathbb{R}^{2n+1} \to \mathbb{R}$ and $\hat{\xi}_t$ is the estimate given by 9. For simplicity, this model is supposed of the same order

as the system (10). The generalization to the case where the order is different is straightforward.

A parametric structure is taken for the function f:

$$f(\cdot) = \sum_{i=1}^{N} \alpha_i \phi_i(\cdot) \tag{12}$$

where $\phi_i : \mathbb{R}^{2n+1} \to \mathbb{R}$ are polynomial basis functions, α_i are parameters to identify. As discussed above, the basis function choice is in general a crucial step, [39], [40], [41]. Here, the motivations for choosing polynomial functions are mainly two: 1) polynomials have proven to be effective approximators in a huge number of problems; 2) as we will see later, they allow a very efficient controller evaluation. A systematic procedure for the choice of the order n, the prediction horizon τ and the polynomial degree is currently under development.

The model parameters α_i are identified from the data (2) by means of convex optimization. Define

$$z \doteq (\tilde{y}_{1+\tau-L}, \ldots, \tilde{y}_0) \in \mathbb{R}^{(L-\tau)\times 1}$$
$$\alpha \doteq (\alpha_1, \ldots, \alpha_N) \in \mathbb{R}^{N\times 1}$$

$$\Phi \doteq \begin{bmatrix} \phi_1\left(\tilde{u}_{1-L}, \tilde{q}_{1-L}^-\right) & \cdots & \phi_N\left(\tilde{u}_{1-L}, \tilde{q}_{1-L}^-\right) \\ \vdots & \ddots & \vdots \\ \phi_1\left(\tilde{u}_{-\tau}, \tilde{q}_{-\tau}^-\right) & \cdots & \phi_N\left(\tilde{u}_{-\tau}, \tilde{q}_{-\tau}^-\right) \end{bmatrix}$$

where $\Phi \in \mathbb{R}^{(L-\tau)\times N}$ and the tilde denotes the samples obtained from the data set (2). Define also the set

$$SC(\gamma, \sigma) \doteq \{\beta \in \mathbb{R}^N : $$
$$|\tilde{y}_{i+\tau} - \tilde{y}_{j+\tau} + (\Phi_j - \Phi_i)\beta|$$
$$\leq \gamma \left\|\tilde{y}_i^- - \tilde{y}_j^-\right\| + 2\sigma, \ j \in \mathcal{T}, i \in \Upsilon_j\}$$

where Φ_k is the kth row of Φ, $\mathcal{T} \doteq \{1-L, \ldots, -\tau\}$, Υ_k is the index set

$$\Upsilon_k \doteq \left\{i : \left\|\left(\tilde{u}_k, \tilde{u}_k^-\right) - \left(\tilde{u}_i, \tilde{u}_i^-\right)\right\| \leq \zeta\right\}$$

and ζ is the minimum value for which every set Υ_k contains at least two elements. Note that SC is defined by a set of linear inequalities in β and σ, and is thus convex in β and σ. In this paper, the following notation for norms is used: $\|\cdot\| \equiv \|\cdot\|_\infty$ is the vector ℓ_∞ norm; $\|\cdot\|_p$ is in general the vector ℓ_p norm.

The vector $\alpha \in \mathbb{R}^N$, whose entries are the parameters of the model (11)-(12), is identified by means of the following convex algorithm. Note that the algorithm is "self-tuning", in the sense that most of the required parameters are automatically chosen, without involving extensive heuristic procedures.

Identification algorithm 2: $\alpha = \mathrm{id\_poly\_1}(DS, \hat{\gamma}_\Delta)$.

Compute α as follows:

1) Solve the preliminary optimization problems

$$\sigma_0 = \min_{\beta \in \mathbb{R}^N} \|z - \Phi\beta\|$$

$$\beta_0 = \arg\min_{\beta \in \mathbb{R}^N} \|\beta\|_1$$
$$\text{s.t.} \quad \|z - \Phi\beta\| \leq \sigma_0 + \rho\|z\|$$

where the ℓ_1 norm and ρ are used to penalize models with high complexity (a simple choice can be $\rho = 0.01$).

2) Solve the optimization problem

$$\begin{aligned} (\alpha, \hat{\sigma}_\Delta) &= \arg\min_{(\beta, \sigma)} \sigma \\ \text{s.t.} \quad \text{(i)} \quad & \beta \in SC(\hat{\gamma}_\Delta, \sigma) \\ \text{(ii)} \quad & \|z - \Phi\beta\|_p \leq \sigma\Lambda \\ \text{(iii)} \quad & \|\beta\|_1 \leq \eta_0 \end{aligned}$$

where $\eta_0 \doteq \|\beta_0\|_1$ and $\Lambda \doteq \frac{\|z-\Phi\beta_0\|_p}{\|z-\Phi\beta_0\|}$. Typical choices of p are $p = 2$ or $p = \infty$.

The rationale of the algorithm can be explained as follows: The goal of step 1 is to initialize several parameters that are needed in step 2. Thanks to step 1, the whole algorithm requires only two inputs: the identification data and $\hat{\gamma}_\Delta$. An optimization problem is then solved in step 2, providing the model parameters. This optimization problem, representing the core of the algorithm, can be explained as follows:

1) The constraint (i) forces the function $\Delta \doteq g - f$ to have a Lipschitz constant non larger than $\hat{\gamma}_\Delta$: a result in [28] shows that this condition can be theoretically guaranteed for a sufficiently large number of data L. On the other hand, Theorem 1 below shows that choosing this constant smaller than 1 allows us to guarantee closed-loop stability.

2) Reducing the prediction error $\|z - \Phi\beta\|_p$ yields a "small" tracking error (the more accurate is the prediction, the more precise is the control action, provided closed-loop stability). Here, a trade-off between stability and tracking performance arises: to satisfy the constraint (i) with $\hat{\gamma}_\Delta < 1$, a large value of $\hat{\sigma}$ may be required, resulting in a large tracking error. Note that any vector norm p in (ii) can be used to reduce the prediction error (typical choices are $p = 2$ or $p = \infty$). Λ is a factor allowing us to normalize, according to the selected ℓ_p norm, the right-hand side of the inequality in (ii).

3) Bounding the ℓ_1 norm leads to a sparse vector α, i.e. a vector with a limited number of non-zero elements, [42], [43], [53], [45]. Sparsity is important to ensure a low model complexity, reducing well known issues such as over-fitting and the curse of dimensionality. Sparsity leads also to an efficient implementation of the model/controller on real-time processors, which may have limited memory and computation capacities. The parameter ρ in step 1 determines the trade-off between model accuracy and sparsity: larger values than 0.01 lead to sparser (but less accurate) models.

VI. CONTROL ALGORITHM AND CLOSED-LOOP STABILITY ANALYSIS

In this section, a control algorithm for nonlinear systems is presented. This algorithm is an extension of the NIC algorithm proposed in [37], [38] to the case where the disturbance estimation is used as an input of the controller

to improve its performance. A closed-loop analysis is also carried out and sufficient stability conditions are derived.

A. Control algorithm

The basic idea of the algorithm is to invert the prediction model (11): at each time $t > 0$, given a reference $r_{t+\tau}$ and the current regressor q_t^-, a command u_t^* is looked for, such that the model output $\hat{y}_{t+\tau}$ is close to $r_{t+\tau}$. Such a command input is found solving the optimization problem

$$u_t^* = \arg \min_{\mathfrak{u} \in U^\tau} J\left(\mathfrak{u}, r_{t+\tau}, q_t^-\right) \tag{13}$$

$$J\left(\mathfrak{u}, r_{t+\tau}, q_t^-\right) \doteq \left(r_{t+\tau} - f\left(\mathfrak{u}, q_t^-\right)\right)^2 + \mu \mathfrak{u}^2 \tag{14}$$

where $q_t^- \doteq \left(u_t^-, y_t^-, \hat{\xi}_t\right)$ and $\hat{\xi}_t$ is the estimate of the unknown disturbance ξ_t in (1) obtained by the estimator (9). The quantity $\mu \geq 0$ is a design parameter, determining the trade-off between tracking precision and command activity. The D2EC control law is fully defined by (13).

It is important to observe that the objective function (14) is in general non-convex. Moreover, the optimization problem (13) has to be solved on-line, and this may take a long time compared to the sampling time used in the application of interest. To overcome these problems, an efficient algorithm is now proposed.

Consider that, for given $r_{t+\tau}$ and q_t^-, the objective function (14) is a polynomial in the scalar variable $\mathfrak{u}$. Its minima can thus be found computing the roots of its derivative, as done in the following algorithm.

Control algorithm 1: $u_t^* = K\left(J, r_{t+\tau}, q_t^-\right)$.

Compute the optimal input as

$$u_t^* = \arg \min_{\mathfrak{u} \in U^s} J\left(\mathfrak{u}, r_{t+\tau}, q_t^-\right) \tag{15}$$

where

$$U^s \doteq \left(\text{Rroots}\left(J'\left(\mathfrak{u}, r_{t+\tau}, q_t^-\right)\right) \cap U\right) \cup \{\underline{u}, \overline{u}\},$$

J' is the derivative of J wrt $\mathfrak{u}$, $\text{Rroots}\left(J'\right)$ denotes the set of all real roots of J', and $\underline{u}$ and $\overline{u}$ are the boundaries of U.

Remark 4: The derivative J' can be computed analytically. Moreover, U^s is composed by a small number of elements:

$$\text{card}\left(U^s\right) < \deg\left(J\left(\mathfrak{u}, r_{t+\tau}, q_t^-\right)\right) + 2$$

where card is the set cardinality and deg indicates the polynomial degree. The evaluation of u^* through Algorithm 1 is thus extremely fast, since it just requires to find the real roots of a univariate polynomial whose analytical expression is known and to compute the objective function for a small number of values. □

The block diagram of the closed-loop system is shown in Figure 1, where "plant" is the system (1), H is the disturbance estimator and K is the controller (13), implemented through the optimization algorithm 1, providing the command input u_t^*.

D2EC can be seen as a particular instance of NMPC, see, e.g., [5], [6], [7]. This is evident from the fact that the command input is chosen on the basis of a prediction model via on-line optimization. However, D2EC has two advantages wrt standard NMPC: 1) It does not need a physical model; 2) it is in general numerically more efficient. Non-standard NMPC approaches that are more similar to D2EC are those presented in [54], [55]. They use polynomial models that can be identified from data, and thus might avoid the need of a physical model. However, these approaches do not give a priori stability/accuracy guarantees. In summary, D2EC can be seen as a data-driven efficient NMPC.

B. Closed-loop stability analysis

In this section, we study the behavior of the closed-loop system formed by the feedback connection of the plant (1), the controller (15) and the estimator (9); that is, the system where the plant (1) is controlled by the input is $u_t = u_t^*$ given by the control law (15), and u_t^* depends on the output of the estimator (9), see Figure 1.

A basic assumption for this closed-loop analysis is that the function h in (1) is Lipschitz continuous on the compact set $U^n \times Y^n$. This assumption is reasonable: a large number of real-world systems are described by functions that are Lipschitz continuous on a compact set. Without loss of generality, we also assume that $U^n \times Y^n$ contains the origin.

Let us now define the functions

$$\Delta\left(q_t^\Delta, y_t^{--}\right) \doteq g\left(u_t^+, u_t^-, y_t^-, \xi_t^v\right) - f\left(u_t, u_t^-, y_t^-, H_t^-\right)$$

$$F\left(r_{t+\tau}, q_t^F, y_t^{--}\right) \doteq r_{t+\tau} - f\left(u_t, u_t^-, y_t^-, H_t^-\right) \tag{16}$$

where

$$H_t^- \doteq (H_{t-1}, \ldots, H_{t-n}) \in \mathbb{R}^n$$
$$H_t \doteq H\left(u_t^-, y_t^-, y_t\right) \in \mathbb{R}$$
$$q_t^\Delta \doteq (u_t^+, u_t^{--}, \xi_t^v) \in Q^\Delta$$
$$q_t^F \doteq (u_t, u_t^{--}) \in Q^F$$
$$y_t^{--} \doteq (y_{t-1}, \ldots, y_{t-2n}) \in \mathbb{R}^{2n}$$
$$u_t^{--} \doteq (u_{t-1}, \ldots, u_{t-2n}) \in U^{2n}.$$

From Lipschitz continuity of h (by assumption) and f (by definition), it follows that Δ and F are Lipschitz continuous on $\Omega_\Delta \doteq Q^\Delta \times Y^{2n}$ and $\Omega_F \doteq Q^F \times Y^{2n+1}$, respectively. Note that Q^Δ and Q^F are compact sets, since q_t^Δ and q_t^F are bounded vectors. From the Lipschitz property, it follows that constants $\gamma_\Delta < \infty$ and $\gamma_F < \infty$ exist such that

$$\gamma_\Delta : \left|\Delta\left(q^\Delta, y\right) - \Delta\left(q^\Delta, y'\right)\right| \leq \gamma_\Delta \|y - y'\|,$$
$$\forall y, y' \in Y^{2n}, \forall q^\Delta \in Q^\Delta$$

$$\gamma_F : \left|F\left(r, u, y\right) - F\left(r, q^F, y'\right)\right| \leq \gamma_F \|y - y'\|,$$
$$\forall y, y' \in Y^{2n}, \forall q^F \in Q^F, \forall r \in Y.$$

Lipschitz continuity of Δ and F in turn implies that constants $\sigma_\Delta < \infty$ and $\sigma_F < \infty$ exist, such that

$$\left|\Delta\left(q_t^\Delta, y_t^{--}\right)\right| \leq \sigma_\Delta$$
$$\left|F\left(r_{t+\tau}, q_t^F, y_t^{--}\right)\right| \leq \sigma_F \tag{17}$$

for any $\boldsymbol{u} = (u_1, u_2, \ldots) \in U^\infty$, any $\boldsymbol{r} = (r_1, r_2, \ldots) \in \mathcal{R}$ and any $\boldsymbol{\xi} = (\xi_1, \xi_2, \ldots) \in \Xi$.

The following result provides sufficient conditions for finite-gain stability of the closed-loop system (1)-(9)-(15) and a worst-case bound on the tracking error.

Theorem 1: Assume that

$$\gamma_c \doteq \gamma_\Delta + \gamma_F < 1 \qquad (18)$$

$$Y \supseteq R \oplus E \qquad (19)$$

where $\oplus$ indicates the set sum, with

$$E \doteq \{\eta \in \mathbb{R}^{n_y} : \|\eta\| \le \bar{e}\}$$

$$\bar{e} \doteq \frac{1}{1-\gamma_c}\left(\sigma_\Delta + \sigma_F + \gamma_\xi \bar{\xi}\right),$$

and γ_ξ is the Lipschitz constant of g wrt ξ_t^v. Then:

(i) The closed-loop system (1)-(9)-(15) is finite-gain ℓ_∞ stable on $(\mathcal{Y}^0, \mathcal{R}, \Xi)$; that is, finite non-negative constants γ_{yr}, $\gamma_{y\xi}$ and λ_y exist such that

$$\|\boldsymbol{y}\| \le \gamma_{yr}\|\boldsymbol{r}\| + \gamma_{y\xi}\|\boldsymbol{\xi}\| + \lambda_y$$

for any $(y_0^-, \boldsymbol{r}, \boldsymbol{\xi}) \in \mathcal{Y}^0 \times \mathcal{R} \times \Xi$.

(ii) The tracking error signal $\boldsymbol{e} = (e_1, e_2, \ldots)$, with $e_t \doteq r_t - y_t$, is bounded as

$$\|\boldsymbol{e}\| \le \bar{e} \qquad (20)$$

for any $(y_0^-, \boldsymbol{r}, \boldsymbol{\xi}) \in \mathcal{Y}^0 \times \mathcal{R} \times \Xi$.

Proof. The proof can be obtained by minor modifications of the proof of Theorem 1 in [38]. $\square$

This theorem shows that two key conditions are sufficient to guarantee closed-loop stability. The first one, i.e., inequality (18), is satisfied if:

(i) $\gamma_\Delta < 1$. This requires the model f to be an accurate approximation of the true function g. In particular, f must be accurate in describing the dependence on y_t (being γ_Δ the Lipschitz constants wrt y_t^{--} of Δ). An important point is that the identification algorithm 2 provides models satisfying this condition when the number of data is sufficiently large, see the discussion below the algorithm.

(ii) $\gamma_F < 1 - \gamma_\Delta$. This condition is satisfied if $\mu = 0$ and $r_{t+\tau}$ is reachable (i.e., in the range of $f\left(\cdot, q_t^-\right)$) for all t. Indeed, in this case, solving problem (13) makes an exact model inversion. That is, $\hat{y}_{t+\tau} = r_{t+\tau}$ for all t, and thus $\gamma_F = 0$. If μ is chosen sufficiently small and $r_{t+\tau}$ is sufficiently close to a reachable value, supposing that γ_F satisfies the assumption is reasonable. On the contrary, if these requirements are not met, condition (18) may be not satisfied, leading to an unstable behavior and possibly to a diverging tracking error. Clearly, if non-reachable trajectories have to be tracked, the only solution is to physically change u_t and/or U, in order to increase the control authority. This means that the actuators of the plant to control have to be changed. The constant γ_F can be estimated from the available data by means of the validation procedure in [50], thus allowing the verification of (18).

The second stability condition, i.e., the set inclusion (19), has a quite intuitive interpretation: It essentially requires the set explored by the data (i.e., Y) to be sufficiently large to contain the set where the trajectories of interest are defined (i.e., R), plus a border region bounded by $\bar{e}$.

VII. BLOOD GLUCOSE REGULATION FOR TYPE 1 DIABETIC PATIENTS - DATA-DRIVEN PATIENT MODELS

Type 1 diabetes (T1DM) is a chronic autoimmune disease characterized by insulin deficiency and resultant hyperglycemia. Insulin is the mainstay of therapy and requires frequent dosing adjustments to maintain a good glycemic control. Despite the advance in care, hypoglycemia and ketoacidosis are persistent potentially life-threatening acute complications in T1DM patients. Hyperglycemia is the primary risk factor for chronic microvascular disease that manifest primarily as retinopathy, neuropathy and nephropathy and can also affect cognitive functions, the heart and other organs.

The concept of Artificial Pancreas (AP) has been introduced, aimed at reducing (or possibly solving) the above problems, offering significant improvements in the life quality of T1DM patients [56]. An AP is a device that controls the blood glucose concentration in diabetic patients. Among the existing AP construction approaches, the closest one to implementation is the so-called medical equipment approach, where the glucose regulation functions of the pancreas are replicated by a fully artificial device. This device incorporates glucose concentration measurements, micro pumps and delivery mechanisms for insulin (and possibly other hormones), and computational and communication devices for implementing a suitable control strategy.

Control of blood glucose concentration has thus a fundamental role in terms of patient wellness and integrity of organs that may be damaged due to T1DM [57], [58], [59], [60], [61]. Control in general implies the availability of reliable models able to predict and/or simulate the behavior of the metabolic system. Different models and modeling techniques have been proposed in the literature, where physiology equations are used to describe the glucose and insulin kinetics in the body [62], [63]. However, although important to understand and analyze the blood glucose dynamics and kinematics, these models cannot in general be very accurate as their equations do not take into account all the dynamics, parameters and disturbances involved in the patient system. Moreover, physiological models do not allow us to properly cope with the high variability among patients.

Nevertheless, the most effective control strategy at present in the diabetes context appears to be MPC (or NMPC). This strategy has already been tested in clinical trials, see, e.g., [64], [65], [66], [67]. The methodologies carried out in these works are valuable and the results obtained in the clinical trials are very promising. However, it seems that the blood glucose regulation results could be further improved, mainly during the day, where the unknown disturbances (meals, emotions, physical activities, ...) strongly affect the metabolic system of diabetic patients (more than during the night).

We think that the D2EC approach presented in this paper may help to obtain some improvement in blood glucose regulation, representing a possible solution to the aforementioned issues (difficult modeling of the pa-

tient, presence of strong unknown disturbances, variability among patients). In the following, after a brief description of the available experimental data, a model of a T1DM patient is identified from a subset of these data. This model, not to be confused with the prediction model of the D2EC algorithm, represents the (unknown) patient, for which a glucose regulator has to be designed. In other words, this patient model is used instead of a real patient (future activities will hopefully be devoted to test the data-driven D2EC approach in clinical trials with real patients). After patient model identification, a disturbance estimator is derived, allowing the estimation of the unknown signals that typically affect a diabetic patient (e.g. food, physical activity, emotions, ...). Next, a D2EC controller for glucose regulation is designed, which takes advantage of the information given by the disturbance estimator. Then, the controller is tested on fresh data, not previously used for model identification and controller/estimator design. Such a procedure is repeated for six different patients and, for each patient, the D2EC controller is compared with other versions of this controller, with a "manual" strategy and with an ideal MPC controller. Finally, a robustness analysis is performed to test if the D2EC controller can work correctly even when some slight change occurs in the dynamics/kinematics of the patient metabolic system.

In a real scenario, the data needed for controller/estimator design can be collected in a preliminary phase of the diabetes treatment, where a "manual" regulation strategy is adopted. For example, in this phase, the insulin can be injected by the patient on the basis of his/hers experience and of the physician indications. After this preliminary phase, the designed controller can be applied to the patient, allowing a fully-automated treatment of T1DM.

A. Experimental datasets

Experimental measurements, collected from six T1DM kid patients, have been considered. The measured input $\tilde{u}_t$ is the rate of insulin injected in the patient body. An insulin pump was used to perform subcutaneous injection of insulin. The measured output $\tilde{y}_t$ is the blood glucose concentration, measured by a Continuous Glucose Monitoring (CGM) sensor Dexcom G4. This sensor worked continuously for about 13 days, procuring a set of 3744 measurements of blood glucose concentration, collected with a sampling time $T_s = 5$ min.

For each patient, the resulting dataset was partitioned in two subsets:

- Identification dataset (first 4 days):

$$IS \doteq \left\{ \tilde{u}_t, \tilde{y}_t \right\}_{t=-1151}^{0}$$

used for model identification and controller design.

- Validation dataset (last 9 days):

$$VS \doteq \left\{ \tilde{u}_t, \tilde{y}_t \right\}_{t=1}^{2592}$$

used for model validation and controller final test.

B. Patient model identification

In the diabetes context, a relevant problem common to all modeling approaches is that a patient is a system affected by unmeasured (or not easily measurable) inputs, and the techniques frequently used for model identification are in general not able to recover or to account for such unmeasured signals. Indeed, modeling of a diabetic patient can be seen as a blind identification problem: not only the patient system has to be identified but also some of its input signals [68].

In this section, we focus on a single T1DM patient, that we call Patient 1. A model of this patient was derived from the identification set IS, using the blind approach shown in Section IV. This approach provides models of the form (1), with estimates of both the function h and the disturbance ξ_t. The model was identified from the Patient 1 identification set IS, and is given by

$$y_t = h_p \left(u_t^-, y_t^- \right) + \hat{\xi}_t^{nc} \tag{21}$$

where u_t is the rate of insulin injected in the patient body, y_t is the patient blood glucose concentration, ξ_t is a disturbance describing the effects of all unknown inputs (e.g. food, physical activity, emotions, etc.), h_p is a function describing the metabolic system kinematics and dynamics. The identified function and disturbance are of the form (3), where $h_p = \hat{h}$ and the parameters were estimated by means of the identification algorithm (8). A model order $n = 9$ has been assumed, since giving the best trade-off between accuracy and complexity (no accuracy improvements were observed for larger orders). Polynomial basis functions χ_i with degree ranging in the interval $[0, 2]$ were considered for the function h. Indeed, no accuracy improvements were observed for larger degrees. On the other hand, a model accuracy degradation was observed on the validation set, using only linear functions (degree 1). Gaussian basis functions $\psi_i (t) = e^{-\beta(t-i)^2}$ were used for the disturbance $\hat{\xi}_t^{nc}$, with $i = 1, \ldots, 1152$ and $\beta = 0.03$ (this value of β was chosen through a trial-and-error procedure).

Several simulations were carried out to test the patient model:

- Simulation 1: The model was performed on the validation set VS, using as inputs the measured insulin signal $\tilde{u}_t$ and the disturbance $\hat{\xi}_t^{nc}$ estimated from the validation set. This estimation was carried out solving the optimization problem (8), only with respect to b, with a fixed and equal to the one previously estimated on the identification set. Figure 2 shows the estimated disturbance (upper plot), the measured insulin input (middle plot), and the output simulated by the model compared with the measured one (bottom plot). The root mean square error resulting from the simulation is $RMSE = 14.4$ mg/dl.
- Simulation 2. For a further verification, the model was tested on completely fresh data (collected in the two days subsequent to the 4 + 9 days already considered). The disturbance $\hat{\xi}_t^{nc}$ was estimated as done for Simulation 1. The results obtained on the fresh data i simulation are similar to those obtained

on the validation set, with a $RMSE$ value equal to 13.9 mg/dl.

- Simulation 3: The model was fed by the disturbance signal $\hat{\xi}_t^{nc}$ estimated from the validation set and by a null insulin input u_t. Being this signal characterized by several positive peaks (presumably corresponding to meals), the output resulting from this simulation became very large, according to a typical hyperglycemia behavior.
- Simulation 4: The model was fed by a null disturbance $\hat{\xi}_t^{nc}$ and by the measured insulin input $\tilde{u}_t$, taken from the validation set. The output moved towards low values, according to a typical hypoglycemia behavior.
- Simulation 5: Starting from an initial output $y_t = 130$ mg/dl, the model was fed by a filtered step disturbance signal $\hat{\xi}_t^{nc}$ of amplitude 1.6 mg/dl and by a small constant insulin input u_t of amplitude 0.2 mg/dl. An increase of about 50 mg/dl, corresponding to the step disturbance, was observed on the output.

All these simulations demonstrate that the identified patient model has a quite reasonable behavior form a physiological point of view.

Note that the patient model is characterized by a gain from the disturbance d_t to the output y_t. This gain can be moved equivalently from the model to the disturbance, without any relevant effect. The disturbance d_t does not describe directly the variations of blood glucose concentration but it is a "virtual" signal that accounts for all disturbances acting on the patient. What is important is that, as verified in the various simulations we have carried out, the effect of this disturbance on the output is realistic.

In the present paper, the model (21) represents the "true" patient for which a glucose regulator has to be designed. This model is assumed unknown (as it happens in a real situation). Only the following data are used for regulator design:

- Design dataset (first 4 days):

$$DS \doteq \{\tilde{u}_t, \tilde{y}_t\}_{t=-1151}^{0}$$

used for estimator and controller design. $\tilde{u}_t$ is the measured insulin signal of IS and $\tilde{y}_t$ is the blood glucose concentration simulated by the patient model (21), fed by $\tilde{u}_t$ and the recovered disturbance signal $\hat{\xi}_t^{nc}$. Note that, in the case where not a patient model but a real patient is under therapy, the sets IS and DS coincide.

C. Disturbance estimator design

A disturbance estimator was designed, whose output was used as an input of the D2EC controllers of Section (VII-D), in order to enhance its performance.

The estimator is of the form (9), with

$$\hat{h}\left(w_t^-\right) = \hat{h}_p\left(u_t^-, y_t^-\right) = \sum_{i=1}^{P} \hat{a}_i \chi_i\left(u_t^-, y_t^-\right)$$

being χ_i polynomial basis functions with maximum degree 2. The parameters $\hat{a}_i$ were estimated from the design set DS by means of the optimization problem in [36]. For this estimator, an order $n = 6$ has been chosen to mimic a real
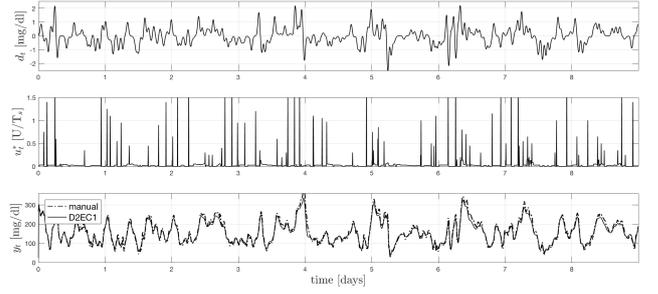

Figure 2. Upper: estimated disturbance. Middle: insulin signal. Lower: comparison between patient model and measured output.

situation, where the order of the true system (i.e., $n = 9$) is not known.

D. Therapy control design

Four controllers for the regulation of blood glucose in Patient 1 were designed (or implemented in the case of the "manual" strategy described below). These controllers are described below, after a schematic summary of the design procedure adopted.

Control design procedure 1

1) *Prediction model identification.* A prediction model is identified from the design set DS, using the identification algorithm 2. The prediction model is of the form (11), with $q_t^- \doteq \left(u_t^-, y_t^-, \hat{\xi}_t^-\right)$, where $\hat{\xi}_t^-$ is the regressor of the on-line disturbance estimate $\hat{\xi}_t$.
2) *Controller design.* From the prediction model identified in step 1, a D2EC controller is designed and implemented, according to the control algorithm 1.
3) *Controller preliminary test.* The controller designed in step 2 is tested in closed-loop on the patient model (21), according to the scheme of Figure 1. The glucose concentration reference value $r_t = 130$ mg/dl, $\forall t$, and the recovered disturbance ξ_t of the design dataset DS are used.
4) *Parameter tuning.* Steps 1-3 are repeated several times considering prediction model orders in the range $[2, 12]$, prediction horizons in the range $[1, 20]$, polynomial degrees in the range $[1, 4]$ and values of μ in the range $[0, 1]$. The parameters providing the best closed-loop performance are chosen. The performance is evaluated through the AUC, AAC and PSI indexes defined below in (22) and (23).

D2EC1 controller. This controller was designed by means of the approach described in the previous sections, following the above procedure to choose the required design parameters. The parameters selected by means of the procedure are: model order $n = 5$, prediction horizon $\tau = 8$, polynomial basis functions up to degree 2, $\mu = 0.1$. Note that the procedure (including prediction model identification, controller design, preliminary test and parameter tuning) only uses data from the design set DS.

D2EC2 controller. This controller is similar to D2EC1 but the prediction model was identified from the set IS, where the output signal is the real one, measured from the patient, and not the one provided by the patient model.

D2EC3 controller. This controller is similar to D2EC1 but the prediction model is linear.

D2C controller. This controller is similar to D2EC1 but the prediction model does not use the disturbance estimation as an input. The prediction model is of the form (11), with $q_t^- \doteq \left(u_t^-, y_t^- \right)$.

Ideal-MPC controller. A nonlinear MPC controller was designed on the basis of the true patient model (21), assuming a prediction horizon $\tau = 8$ (as done for the D2EC1 controller). This controller uses the true disturbance signal as an input. The true disturbance is used in a non-causal way, in the sense that, at a given time, past, current and future disturbance values are assumed to be known. Clearly, this is an ideal controller that cannot be implemented in a real situation, where the true model and disturbance are not known. Nevertheless, this controller is useful as a term of comparison, to individuate the ideal performance that could be attained in the present setting, under the non-realistic assumption that the true system and disturbance are known.

Manual Controller. A "manual" regulation strategy was implemented, where the insulin is injected by the patient on the basis of his/hers experience and possibly of the indications coming from a semi-automated glucose regulation device. To be close to a real situation, the measured insulin signal $\tilde{u}_t$ of the validation set VS was used for this purpose.

E. Blood glucose regulation for a diabetic patient

The controllers designed in Section VII-D were tested on the model of Patient 1, according to the scheme of Figure 1. In the figure, "plant" is the patient model (21), H is the disturbance estimator, K is the controller, y_t is the patient blood glucose concentration, r_t is a desired reference value, u_t^* is the insulin rate, ξ_t is a disturbance describing the effects of all unknown inputs (e.g. food, physical activity, emotions, etc.) and $\hat{\xi}_t$ is the disturbance estimate. The glucose concentration reference value $r_t = 130$ mg/dl, $\forall t$, was imposed, and the recovered disturbance ξ_t of the validation set VS was used. This disturbance was obtained solving the optimization problem (8) only with respect to b, being a the coefficient vector of of the already identified model $\hat{h}_p$.

Typically, the goal of regulation is too keep the value of the blood glucose concentration y_t inside the interval $[70, 180]$ mg/dl which, in diabetes treatment medicine, is commonly considered a safe interval. Thus, the following indexes were used to measure the quality of the treatment:

$$
\begin{aligned}
AUC &\doteq \tfrac{1}{L_V} \sum_{t=1}^{L_V} (y_t < 70)(70 - y_t) \\
AAC &\doteq \tfrac{1}{L_V} \sum_{t=1}^{L_V} (y_t > 180)(y_t - 180)
\end{aligned}
\tag{22}
$$

where $(y_t < 70)$ and $(y_t > 180)$ are logical operators and L_V is the validation data set length. These indexes,

called *area under the curve* (AUC) and *area above the curve* (AAC), respectively, measure the amount of glucose exceeding the bounds. Another index that is commonly used is the percentage of time (or samples) spent in the safe interval [69], defined as

$$
PSI \doteq \frac{100 \, \mathrm{card}\{t \in [1, L_V] : 70 \leq y_t \leq 180\}}{L_V}
\tag{23}
$$

where card is the set cardinality. A more complete set of metrics (including the PSI index) has been identified by members of the JDRF Artificial Pancreas Project Consortium, in collaboration with other representatives of the AP community, to measure the effectiveness of blood glucose control algorithms [69]. For the sake of brevity, within this set, only the PSI index is considered in the present study. The values of the AUC, AAC and PSI indexes obtained by the control therapy strategies, with the disturbance ξ_t of the validation set VS affecting the patient model, are reported in Table I. The glucose concentration signals for the D2EC1 and manual strategies are shown in Figure 4 (bottom plot). In the figure, also the corresponding disturbance and insulin input signals are shown (upper and middle plot), where the insulin input is given by the D2EC1 controller. A comparison between the true and estimated disturbance is shown in Figure 3, for a portion of the validation set. It can be noted that the estimated disturbance has a delay wrt the true one but it is able to capture its behavior quite effectively.

These results demonstrate that the D2EC strategies are effective in regulating the blood glucose concentration of the identified patient model, yielding significantly lower values of AAC and higher values of PSI with respect to the manual strategy. Note that the manual strategy is a real one, actually applied to a real diabetic patients, and the dot-dashed signal in Figure 4 (bottom plot) represents quite accurately what happened to the blood glucose concentration in the real patient. The D2EC1 strategy is not far from the ideal strategy and both of them are quite better than the others. This demonstrates that (i) using a nonlinear prediction model helps to improve the control performance (this is reasonable, since the patient model is nonlinear); (ii) using the estimated disturbance helps to improve the control performance. The D2EC2 strategy also provides satisfactory results (although not the best ones), thus showing interesting robustness properties: the strategy worked well when applied to the patient model even if the data used for its design where produced by a different patient (the true human patient). This situation should not occur in a real application of a D2EC strategy, since a D2EC therapy control applied to a real patient should be designed from data generated by the same patient (personalized therapy). However, if the patient glucose dynamics and/or kinematics change for some unexpected reason, robustness is important to ensure that the therapy control in any case continues to work (even if not at best), regulating the blood glucose concentration so to avoid hypoglycemia or hyperglycemia phenomena. A more exhaustive robustness analysis, involving 50 different patient models, is carried out in Section VII-G.

	AUC	AAC	PSI
D2EC1	0.069	0.505	95
D2EC2	0.064	2.634	88
D2EC3	0.061	2.914	86
D2C	0.102	1.759	92
Ideal-MPC	0.067	0.107	98
Manual	0.100	13.762	66

Table I
DIABETES TREATMENT RESULTS FOR A PATIENT (DATA-DRIVEN MODEL).

	AUC_{avg}	AAC_{avg}	PSI_{avg}
D2EC1	0.066	0.508	95
D2EC2	0.067	2.687	88
D2EC3	0.064	2.914	86
D2C	0.111	1.789	92
Ideal-MPC	0.063	0.486	98
Manual	0.101	13.101	67

Table II
DIABETES TREATMENT QUALITY FOR FIVE PATIENTS (DATA-DRIVEN MODEL). AVERAGE PERFORMANCE INDEXES.
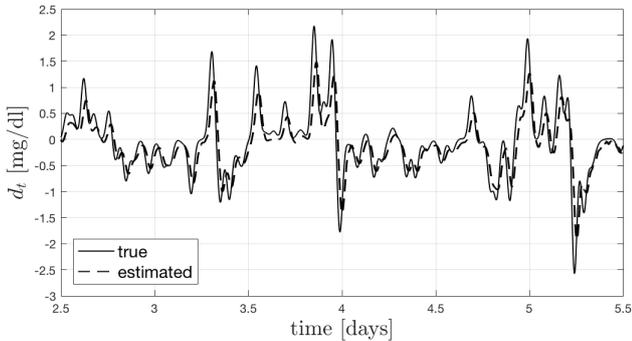
Figure 3. Disturbance on-line estimation.

	AUC_{wc}	AAC_{wc}	PSI_{wc}
D2EC1	0.073	0.621	93
D2EC2	0.074	2.913	86
D2EC3	0.072	3.243	85
D2C	0.155	1.961	91
Ideal-MPC	0.067	0.579	98
Manual	0.135	15.002	64

Table III
DIABETES TREATMENT QUALITY FOR FIVE PATIENTS (DATA-DRIVEN MODEL). WORST-CASE PERFORMANCE INDEXES.

It is important to remark that the AUC values cannot be reduced significantly, because insulin only allows us to decrease the blood glucose concentration but not to increase it. In other words, this input can only regulate the glucose concentration in one direction. Improvements in terms of AUC reduction may be expected using additional control inputs, such as Glucagon, which, together with insulin, may enable the controller to regulate the glucose in two directions.

F. Blood glucose regulation for 5 patients

All the operations described in Sections VII-B-VII-E have been repeated for other 5 diabetic patients. In particular, for each patient, a model was identified representing his/her blood glucose behavior. A disturbance estimator was designed from the data generated by the patient model. Six controllers/strategies (D2EC1-D2EC3, D2C, ideal-MPC and manual) where designed/implemented, as done in Section VII-D. Then, all these controllers were tested in closed-loop on the patient model, using disturbance signals estimated from the validation set. The AUC, AAC and PSI indexes, averaged over the 5 patients, are reported in Table II. The worst-case values obtained for these indexes are shown in Table III.

These results confirm what obtained for the first patient and show that the D2EC approach can provide quite uniform results, when applied to different diabetic patients. An important aspect is that the approach allows a personalized treatment for each patient, where the insulin delivery strategy is synthesized from the data that contain a relevant information about the patient metabolic system behavior.

G. Robustness analysis

The patient model identification procedure of Section VII-B was repeated for 50 trials, considering different model orders, polynomial degrees and disturbance basis functions. In particular, in each trial, we assumed a model order chosen randomly in the range $[7, 11]$, a polynomial degree chosen randomly in the range $[1, 4]$, and a coefficient β (appearing in the disturbance basis functions) chosen randomly in the range $[0.01, 0.05]$. From these trials, a set of 50 different models was obtained, representing a set of 50 perturbations of a diabetic patient. Then, the D2EC1 control strategy designed in Section VII-D was tested on all these models. Note that the controller was not re-designed for each model but was always the same. This kind of test is interesting to assess the robustness properties of the controller. As discussed above, robustness may be important when the patient glucose dynamics and/or kinematics slightly change for some unexpected reason. In this case, robustness can ensure that the therapy control continues to properly regulate the blood glucose concentration (although not in an optimal way), avoiding dangerous hypoglycemia or hyperglycemia phenomena. Clearly, once the change of dynamics and/or kinematics has been detected, a new D2EC strategy have to be designed, in order to restore an optimal regulation of the blood glucose.

The AUC, AAC and PSI indexes, averaged over the 50 patients, are reported in Table IV. The worst-case values obtained for these indexes are shown in Table (V).

These results confirm what obtained above by the D2EC2 strategy: they show that a D2EC therapy control strategy can be quite robust versus possible slight changes in the patient metabolic system.

	AUC_{avg}	AAC_{avg}	PSI_{avg}
D2EC1	0.083	3.711	83

Table IV
ROBUSTNESS TEST FOR THE D2EC1 STRATEGY (DATA-DRIVEN MODEL). AVERAGE PERFORMANCE INDEXES.

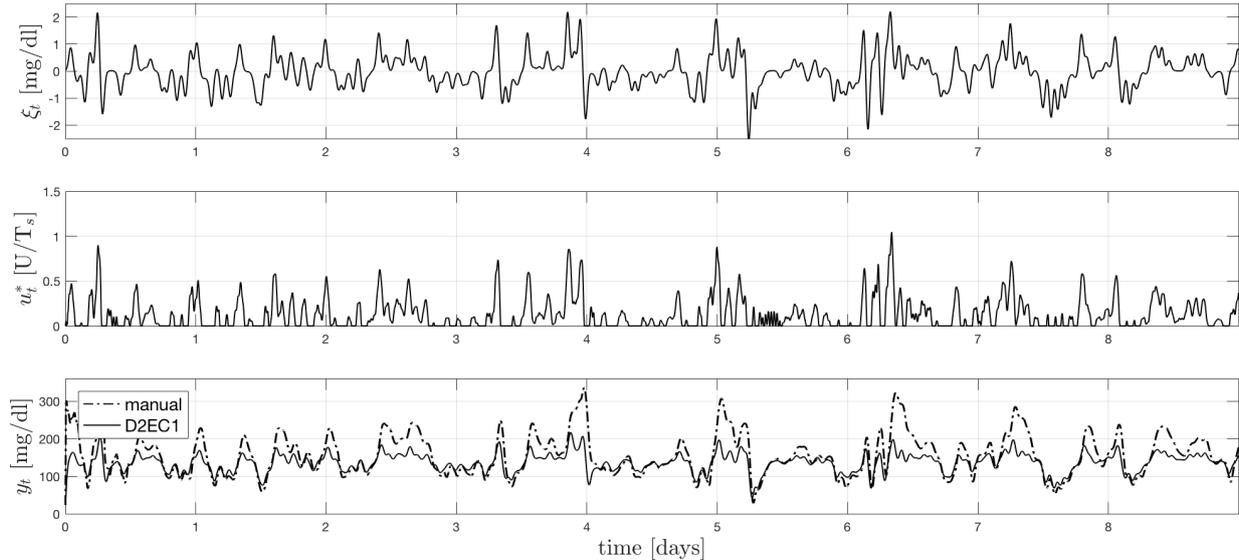Figure 4. Diabetes treatment results for a patient (data-driven model).

	AUC_{wc}	AAC_{wc}	PSI_{wc}
D2EC1	0.094	4.273	79

Table V
ROBUSTNESS TEST FOR THE D2EC1 STRATEGY (DATA-DRIVEN MODEL). WORST-CASE PERFORMANCE INDEXES.

VIII. BLOOD GLUCOSE REGULATION FOR A TYPE 1 DIABETIC PATIENT - PHYSIOLOGICAL PATIENT MODEL

In this section, the D2EC approach is tested on the simulator of a Type 1 diabetic patient presented in [70], called here T1DMS (Type 1 diabetes metabolic simulator). The simulator is obtained from a revised version of the well-known UVA/Padova model, a world-recognized benchmark tool for testing blood glucose regulation algorithms, also approved by the Food and Drug Administration (FDA) [71].

T1DMS is a quite complex physiological model, accounting for several aspects of the metabolic process, and is composed by several subsystems such as: glucose subsystem, insulin subsystem, glucose rate of appearance, endogenous glucose production, glucose utilization, renal excretion, subcutaneous insulin kinetics, subcutaneous glucose kinetics, glucagon kinetics and secretion, subcutaneous glucagon kinetics and glucose sensor model (with measurement errors). In [70], all the T1DMS equations are summarized and simulation results are reported, validating the simulator in comparison with the UVA/Padova model. The equations are not reported here for the sake of brevity. In this section, T1DMS is also called the "patient model" and is assumed to be unknown.

A simulation of the patient model corresponding to a duration 13 days was carried out and a set of input-output data was collected with a sampling time $T_s = 1$ min. The output $\tilde{y}_t$ is the blood glucose concentration. The input $\tilde{u}_t$ is the rate of insulin injected in the patient body, modeled as a constant signal (basal dose) plus a sequence of square signals of short duration, corresponding to insulin

injections. The patient model was also affected by a disturbance ξ_t (assumed to be not measured), representing the rate of ingested carbohydrates, modeled as a sequence of impulsive signals, each corresponding to a meal. The signals $\tilde{u}_t$ and ξ_t used here are similar to those used in [70] in terms amplitude, duration and frequency of occurrence of injections and meals. The total dataset was partitioned in two subsets:

• Design dataset (first 4 days):

$$DS \doteq \left\{ \tilde{u}_t, \tilde{y}_t \right\}_{t=-5759}^{0}$$

used for estimator/controller design.

• Validation dataset (last 9 days):

$$VS \doteq \left\{ \tilde{u}_t, \tilde{\tilde{y}}_t \right\}_{t=1}^{12960}$$

used for estimator/controller test.

The operations described in Sections VII-C-VII-E have been repeated using these data. In particular, a disturbance estimator with order 6 and polynomial basis functions with maximum degree 2 was designed. Two controllers (D2EC1 and manual) where then designed/implemented, as done in Section VII-D. The two controllers are the following:

D2EC1 controller. This controller was designed by means of the D2EC approach from the design dataset, following the procedure of Section VII-D to choose the required design parameters. The parameters selected by means of the procedure are: model order $n = 8$, prediction horizon $\tau = 90$, polynomial basis functions up to degree 2, $\mu = 0.1$. Note that here the controller sampling time is $T_s = 1$ min.

Manual Controller. A "manual" regulation strategy was implemented, where the insulin is injected by the patient on the basis of his/hers experience and possibly of the indications coming from a semi-automated glucose regulation device. Here, insulin and meal signals were chosen similar to the ones of [70]. Note that these input signals applied

	AUC	AAC	PSI
D2EC1	0.053	1.975	89
Manual	0.033	13.329	72

Table VI

DIABETES TREATMENT RESULTS FOR A PATIENT (UVA/PADOVA MODEL).

to the patient model provided an output signal $\tilde{y}_t$ quite realistic, with a behavior close to the one observed from the real data of Section VII-A.

The two controllers were tested on the patient model (T1DMS), using the validation dataset. The resulting AUC, AAC and PSI indexes are reported in Table VI. The glucose concentration signals for the D2EC1 and manual strategies are shown in Figure 5 (bottom plot). In the figure, also the corresponding disturbance and insulin input signals are shown (upper and middle plot), where the insulin input is given by the D2EC1 controller.

These results are similar to those obtained in Section VII-E, confirming that the D2EC approach can be effective, also when applied to a patient model based on first-principle equations, characterized by a completely different model structure and a completely different class of nonlinearities with respect to those used by D2EC for estimation and control.

Clearly, the simulation made here with T1DMS represents a preliminary study. Future research activities will be dedicated to run extensive Monte Carlo simulations using the UVA/Padova simulator, where different patients and scenarios will be considered, investigating relevant properties, such as robustness (versus small patient perturbations), sensitivity to noises/errors and trade-off between personalization and robustness.

IX. CONCLUSIONS

An approach to nonlinear system control has been presented, based on three main steps: In the first step (off-line), a disturbance estimator is designed from data. In the second step (off-line), a prediction model for the plant to control is identified from the same data. In the third step (on-line), the control law is obtained by inversion of the prediction model, via efficient optimization.

The approach has been applied to a real data case study, regarding insulin regulation in type 1 diabetic patients. It has also been preliminarily tested using a diabetic patient simulator, obtained from a revised version of the well-known UVA/Padova model. In both the real data and simulator studies, the results indicate that the approach could

become a useful tool in the context of diabetes treatment. It must be remarked that these results are preliminary and further validations are needed before testing the approach in clinical trials. In this view, future activities will be dedicated to (i) running extensive Monte Carlo simulations using the UVA/Padova simulator; (ii) developing estimators with a NARMAX structure; (iii) performing hardware-in-the-loop tests of the D2EC approach; (iv) in the case of success in all the tests and simulations, using if possible the D2EC approach in clinical trials.

REFERENCES

[1] A. Isidori, *Nonlinear Control Systems*. Springer, 1995.

[2] L. Freidovich and H. Khalil, "Performance recovery of feedback-linearization-based designs," *IEEE Transactions on Automatic Control*, vol. 53, no. 10, pp. 2324 – 2334, 2008.

[3] S. Battilotti, "Robust stabilization of nonlinear systems with point-wise norm-bounded uncertainties: a control Lyapunov function approach," *IEEE Transactions on Automatic Control*, vol. 44, no. 1, pp. 3 – 17, 1999.

[4] S. Nersesov and M. Haddad, "On the stability and control of nonlinear dynamical systems via vector Lyapunov functions," *IEEE Transactions on Automatic Control*, vol. 51, no. 2, pp. 203 – 215, 2006.

[5] "Assessment and future directions of nonlinear model predictive control," in *Lecture Notes in Control and Information Sciences*, R. Findeisen, F. Allgower, and L. Biegel, Eds. Springer, 2007.

[6] "Nonlinear model predictive control - towards new challenging applications," in *Lecture Notes in Control and Information Sciences*, L. Magni, D. Raimondo, and F. Allgower, Eds. Springer, 2009.

[7] "Nonlinear model predictive control - theory and algorithms," in *Communications and Control Engineering*, L. Grune and J. Pannek, Eds. Springer, 2011.

[8] A. Freeman and V. Kokotovic, *Robust Nonlinear Control Design*. Boston: Birkhï¿œuser, 1996.

[9] Z. Qu, *Robust Control of Nonlinear Uncertain Systems*. Wiley series in nonlinear science, 1998.

[10] B. Yao and M. Tomizuka, "Adaptive robust control of mimo nonlinear systems in semi-strict feedback forms," *Automatica*, vol. 37, 2001.

[11] J. Chen and G. Gu, *Control-Oriented System Identification: An H_∞ Approach*. New York: John Wiley & Sons, 2000.

[12] Z. Gao, "On the centrality of disturbance rejection in automatic control," *ISA Transactions*, vol. 53, no. 4, pp. 850–857, 2014.

[13] C. Novara, E. Canuto, and D. Carlucci, "Control of systems with sector-bounded nonlinearities: robust stability and command effort minimization by disturbance rejection," *Control Theory and Technology*, vol. 14, no. 3, pp. 209–223, 2016.

[14] K. S. Narendra and K. Parthasarathy, "Identification and control of dynamical systems using neural networks," *IEEE Transaction on Neural Networks*, vol. 1, no. 1, pp. 4–27, 1990.

[15] F.-C. Chen and H. Khalil, "Adaptive control of a class of nonlinear discrete-time systems using neural networks," *IEEE Transactions on Automatic Control*, vol. 40, no. 5, pp. 791–801, 1995.

[16] K. J. Astrom and B. Wittenmark, *Adaptive Control*. Reading, MA: Addison-Wesley, 1995.

[17] A. Levin and K. Narendra, "Control of nonlinear dynamical systems using neural networks. II. observability, identification, and control," *IEEE Transaction on Neural Networks*, vol. 7, no. 1, pp. 30–42, 1996.

[18] M. Polycarpou, "Stable adaptive neural control scheme for nonlinear systems," *IEEE Transactions on Automatic Control*, vol. 41, no. 3, pp. 447–451, 1996.

[19] J. Cabrera and K. S. Narendra, "Issues in the application of neural networks for tracking based on inverse control," *IEEE Transactions on Automatic Control*, vol. 44, no. 11, pp. 2007–2027, 1999.

[20] K. J. Hunt and D. Sbarbaro, "Neural networks for nonlinear internal model control," *Control Theory and Applications, IEE Proceedings D*, vol. 138, no. 5, pp. 431–438, 1991.

[21] M. Brown, G. Lightbody, and G. Irwin, "Nonlinear internal model control using local model networks," *IEE Proceedings - Control Theory and Applications*, vol. 144, no. 6, pp. 505–514, 1997.

[22] C. Novara, M. Canale, M. Milanese, and M. Signorile, "Set Membership inversion and robust control from data of nonlinear systems," *International Journal of Robust and Nonlinear Control*, vol. 24, no. 18, pp. 3170–3195, 2014.
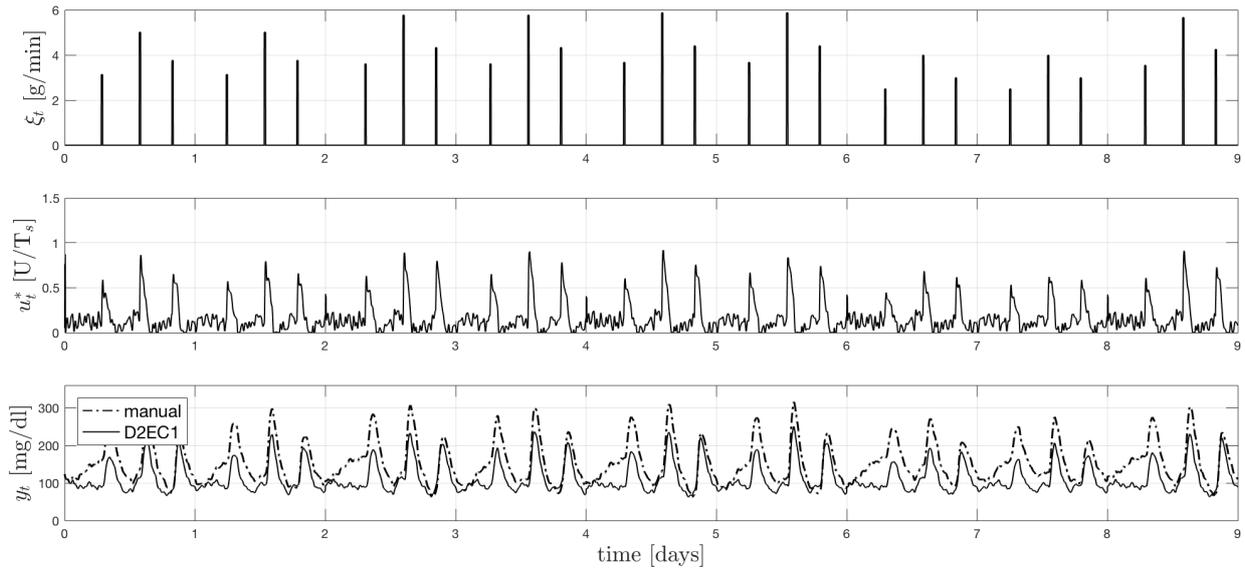
Figure 5. Diabetes treatment results for a patient (UVA/Padova model).

[23] G. Bontempi, M. Birattari, and H. Bersini, "Lazy learning for local modelling and control design," *International Journal of Control*, 1999.

[24] A. Yesildirek and L. Lewis, "Feedback linearization using neural networks," *Automatica*, vol. 31, no. 11, pp. 1659–1664, 1995.

[25] G. C. M. D. Abreu, R. L. Teixeira, and J. F. Ribeiro, "A neural network-based direct inverse control for active control of vibrations of mechanical systems," in *Proceedings of the sixth Brazilian Symposium on Neural Networks*, 2000, pp. 107–112.

[26] M. Campi and S. Savaresi, "Direct nonlinear control design: The virtual reference feedback tuning (VRFT) approach," *IEEE Transactions on Automatic Control*, vol. 51, no. 1, pp. 14–27, 2006.

[27] D. B. Anuradha, G. P. Reddy, and J. S. N. Murthy, "Direct inverse neural network control of a continuous stirred tank reactor (cstr)," in *Proceedings of the International MultiConference of Engineers and Computer Scientists*, Hong Kong, 2009.

[28] C. Novara, L. Fagiano, and M. Milanese, "Direct feedback control design for nonlinear systems," *Automatica*, vol. 49, no. 4, pp. 849–860, 2013.

[29] L. Fagiano and C. Novara, "Learning a nonlinear controller from data: theory, computation and experimental results," *IEEE Transactions on Automatic Control*, vol. 61, no. 7, pp. 1854–1868, 2016.

[30] Z. Hou and S. Jin, "A novel data-driven control approach for a class of discrete-time nonlinear systems," *IEEE Transactions on Control Systems Technology*, vol. 19, no. 6, pp. 1549–1558, 2011.

[31] ——, "Data-driven model-free adaptive control for a class of mimo nonlinear discrete-time systems," *IEEE Transactions on Neural Networks*, vol. 22, no. 12, pp. 2173–2188, Dec 2011.

[32] F. Lewis, D. Vrabie, and K. Vamvoudakis, "Reinforcement learning and feedback control: Using natural decision methods to design optimal adaptive controllers," *Control Systems, IEEE*, vol. 32, no. 6, pp. 76–105, 2012.

[33] S. Yin, H. Luo, and S. Ding, "Real-time implementation of fault-tolerant control systems with performance optimization," *IEEE Transactions on Industrial Electronics*, vol. 61, no. 5, pp. 2402–2411, 2014.

[34] D. Xu, B. Jiang, and P. Shi, "A novel model-free adaptive control design for multivariable industrial processes," *IEEE Transactions on Industrial Electronics*, 2014.

[35] J. C. Spall, "Adaptive stochastic approximation by the simultaneous perturbation method," *IEEE Transactions on Automatic Control*, 2000.

[36] C. Novara, N. Pour, T. Vincent, and G. Grassi, "A nonlinear blind identification approach to modeling of diabetic patients," *IEEE Transactions on Control Systems Technology*, vol. 24, no. 3, pp. 1092–1100, 2016.

[37] C. Novara, S. Formentin, S. Savaresi, and M. Milanese, "Data-driven design of two degree-of-freedom nonlinear controllers: the D2-IBC approach," *Automatica*, vol. 72, pp. 19–27, 2016.

[38] C. Novara and S. Formentin, "Data-driven inversion-based control of nonlinear systems with guaranteed closed-loop stability," *IEEE Transactions on Automatic Control*, in press, doi:10.1109/TAC.2017.2744499.

[39] J. Sjöberg, Q. Zhang, L. Ljung, A. Benveniste, B.Delyon, P. Glorennec, H. Hjalmarsson, and A. Juditsky, "Nonlinear black-box modeling in system identification: a unified overview," *Automatica*, vol. 31, pp. 1691–1723, 1995.

[40] K. Hsu, C. Novara, T. Vincent, M. Milanese, and K. Poolla, "Parametric and nonparametric curve fitting," *Automatica*, vol. 42/11, pp. 1869–1873, 2006.

[41] C. Novara, T. Vincent, K. Hsu, M. Milanese, and K. Poolla, "Parametric identification of structured nonlinear systems," *Automatica*, vol. 47, no. 4, pp. 711 – 721, 2011.

[42] R. Tibshirani, "Regression shrinkage and selection via the Lasso," *Royal. Statist. Soc B.*, vol. 58, no. 1, pp. 267–288, 1996.

[43] D. Donoho, M. Elad, and V. Temlyakov, "Stable recovery of sparse overcomplete representations in the presence of noise," *IEEE Transactions on Information Theory*, vol. 52, no. 1, pp. 6 – 18, jan. 2006.

[44] E. Candes and T. Tao, "Near-optimal signal recovery from random projections: Universal encoding strategies?" *IEEE Transactions on Information Theory*, vol. 52, no. 12, pp. 5406 –5425, dec. 2006.

[45] J. Tropp, "Just relax: convex programming methods for identifying sparse signals in noise," *IEEE Transactions on Information Theory*, vol. 52, no. 3, pp. 1030 –1051, mar. 2006.

[46] M. Milanese, J. Norton, H. P. Lahanier, and E. Walter, *Bounding Approaches to System Identification*. Plenum Press, 1996.

[47] F. Ruiz, C. Novara, and M. Milanese, "Direct design from data of optimal filters for LPV systems," *Systems and Control Letters*, vol. 59/1, pp. 1–8, 2010.

[48] M. Milanese and C. Novara, "Unified set membership theory for identification, prediction and filtering of nonlinear systems," *Automatica*, vol. 47, no. 10, pp. 2141–2151, 2011.

[49] C. Novara, F. Ruiz, and M. Milanese, "Direct filtering: a new approach to optimal filter design for nonlinear systems," *IEEE Transactions on Automatic Control*, vol. 58, no. 1, pp. 86–99, 2013.

[50] M. Milanese and C. Novara, "Set membership identification of nonlinear systems," *Automatica*, vol. 40/6, pp. 957–975, 2004.

[51] J. Fuchs, "Recovery of exact sparse representations in the presence of bounded noise," *IEEE Transactions on Information Theory*, vol. 51, no. 10, pp. 3601 –3608, oct. 2005.

[52] C. Novara, "Sparse identification of nonlinear functions and parametric set membership optimality analysis," *IEEE Transactions on Automatic Control*, vol. 57, no. 12, pp. 3236–3241, 2012.

[53] E. Candes, J. Romberg, and T. Tao, "Robust uncertainty principles: exact signal reconstruction from highly incomplete frequency information," *IEEE Transactions on Information Theory*, vol. 52, no. 2, pp. 489 – 509, feb. 2006.

[54] G. R. Sriniwas and Y. Arkun, "A global solution to the nonlinear model predictive control algorithms using polynomial arx models," *Computers and Chemical Engineering*, vol. 21, no. 4, pp. 431–439, 1997.

[55] R. Parker, "Nonlinear model predictive control of a continuous bioreactor using approximate data-driven models," in *American Control Conference*, Anchorage, AK, USA, 2002.

[56] T. Hampton, "Fully automated artificial pancreas finally within reach," *Jama*, vol. 311, no. 22, pp. 2260–2261, 2014.

[57] R. Harvey, Y. Wang, B. Grosman, M. Percival, W. Bevier, D. Finan, H. Zisser, D. Seborg, L. Jovanovic, F. Doyle, and E. Dassau, "Quest for the artificial pancreas: Combining technology with treatment," *Engineering in Medicine and Biology Magazine, IEEE*, vol. 29, no. 2, pp. 53–62, 2010.

[58] C. Cobelli, E. Renard, and B. Kovatchev, "Artificial pancreas: Past, present, future," *Diabetes*, vol. 60, pp. 2672–2682, 2011.

[59] B. W. Bequette, "Challenges and recent progress in the development of a closed-loop artificial pancreas," *Annual Reviews in Control*, vol. 36, no. 2, pp. 255 – 266, 2012.

[60] J. B. Lee, E. Dassau, D. Seborg, and F. Doyle, "Model-based personalization scheme of an artificial pancreas for type 1 diabetes applications," in *American Control Conference (ACC), 2013*, June 2013, pp. 2911–2916.

[61] "JDRF artificial pancreas project," http://artificialpancreasproject.com/.

[62] I. Ajmera, M. Swat, C. Laibe, N. Le Novère, and V. Chelliah, "The impact of mathematical modeling on the understanding of diabetes and related complications," *CPT: Pharmacometrics & Systems Pharmacology*, vol. 2, p. e54, 2013.

[63] S. Dube, I. Errazuriz, C. Cobelli, R. Basu, and A. Basu, "Assessment of insulin action on carbohydrate metabolism: Physiological and non-physiological methods," *Diabetic Medicine*, vol. 30, no. 6, pp. 664–670, 2013.

[64] S. Patek, L. Magni, E. Dassau, C. Hughes, C. Toffanin, G. D. Nicolao, M. Breton, C. D. Man, E. Renard, H. Zisser, F. D. III, C. Cobelli, and B. Kovatchev, "Modular closed-loop control of diabetes," *IEEE Transactions on Biomedical Engeneering*, vol. 59, no. 11, pp. 2986–2999, 2012.

[65] J. Kropff, S. D. Favero, J. Place, C. Toffanin, R. Visentin, M. Monaro, M. Messori, F. D. Palma, G. Lanzola, A. Farret, F. Boscari, S. Galasso, P. Magni, A. Avogaro, P. Keith-Hynes, B. P. Kovatchev, D. Bruttomesso, C. Cobelli, J. H. DeVries, E. Renard, and L. Magni, "2 month evening and night closed-loop glucose control in patients with type 1 diabetes under free-living conditions: a randomised crossover trial," *Lancet Diabetes Endocrinol*, vol. 3, no. 12, pp. 939–947, 2015.

[66] R. Gondhalekar, E. Dassau, and F. D. III, "Velocity-weighting to prevent controller-induced hypoglycemia in mpc of an artificial pancreas to treat t1dm," in *Proc. of American Control Conference*, 2015, pp. 1635–1640.

[67] C. Toffanin, M. Messori, C. Cobelli, and L. Magni, "Automatic adaptation of basal therapy for type 1 diabetic patients: a run-to-run approach," *Biomedical Signal Processing and Control*, vol. 31, pp. 539–549, 2017.

[68] K. Abed-Meraim, W. Qiu, and Y. Hua, "Blind system identification," *Proceedings of the IEEE*, vol. 85, no. 8, pp. 1310–1322, 1997.

[69] D. Maahs, B. Buckingham, J. Castle, A. Cinar, E. Damiano, E. Dassau, J. Hans De Vries, F. Doyle, S. Griffen, A. Haidar, L. Heinemann, R. Hovorka, T. Jones, C. Kollman, B. Kovatchev, B. Levy, R. Nimri, D. O'Neal, M. Philip, E. Renard, S. Russell, S. Weinzimer, H. Zisser, and J. Lum, "Outcome measures for artificial pancreas clinical trials: A consensus report," *Diabetes Care*, 2016.

[70] A. Molano-Jimenez and F. Leon-Vargas, "UVa/Padova T1DMS dynamic model revision: For embedded model control," in *2017 IEEE 3rd Colombian Conference on Automatic Control, CCAC 2017*. https://ieeexplore.ieee.org/stamp/stamp.jsp?tp=&arnumber=8276390, 2018.

[71] R. Visentin, E. Campos-Náñez, M. Schiavon, D. Lv, M. Vettoretti, M. Breton, B. P. Kovatchev, C. Dalla Man, and C. Cobelli, "The UVA/Padova Type 1 Diabetes Simulator Goes From Single Meal to Single Day," *Journal of Diabetes Science and Technology*, 2018.